# Rapid, efficient functional characterization and recovery of HIV-specific human CD8$^+$ T cells using microengraving

Navin Varadarajan[a,1,2], Douglas S. Kwon[b,c,2], Kenneth M. Law[b], Adebola O. Ogunniyi[a], Melis N. Anahtar[b], James M. Richter[d], Bruce D. Walker[b,e], and J. Christopher Love[a,b,3]

[a]Department of Chemical Engineering, Koch Institute for Integrative Cancer Research, Massachusetts Institute of Technology, Cambridge, MA 02139; [b]The Ragon Institute of Massachusetts General Hospital, Massachusetts Institute of Technology, and Harvard University, Charlestown, MA 02129; Divisions of [c]Infectious Diseases and [d]Gastroenterology, Massachusetts General Hospital, Boston, MA 02114; and [e]Howard Hughes Medical Institute, Chevy Chase, MD 20815

Edited by Herman N. Eisen, Massachusetts Institute of Technology, Cambridge, MA, and approved January 25, 2012 (received for review July 11, 2011)

**The nature of certain clinical samples (tissue biopsies, fluids) or the subjects themselves (pediatric subjects, neonates) often constrain the number of cells available to evaluate the breadth of functional T-cell responses to infections or therapeutic interventions. The methods most commonly used to assess this functional diversity ex vivo and to recover specific cells to expand in vitro usually require more than $10^6$ cells. Here we present a process to identify antigen-specific responses efficiently ex vivo from $10^4$–$10^5$ single cells from blood or mucosal tissues using dense arrays of subnanoliter wells. The approach combines on-chip imaging cytometry with a technique for capturing secreted proteins—called "microengraving"—to enumerate antigen-specific responses by single T cells in a manner comparable to conventional assays such as ELISpot and intracellular cytokine staining. Unlike those assays, however, the individual cells identified can be recovered readily by micromanipulation for further characterization in vitro. Applying this method to assess HIV-specific T-cell responses demonstrates that it is possible to establish clonal CD8$^+$ T-cell lines that represent the most abundant specificities present in circulation using 100- to 1,000-fold fewer cells than traditional approaches require and without extensive genotypic analysis a priori. This rapid (<24 h), efficient, and inexpensive process should improve the comparative study of human T-cell immunology across ages and anatomic compartments.**

T-cell cloning | single-cell analysis | nanowells | microarrays | soft lithography

CD8$^+$ T cells are a critical component of the adaptive immune system and provide immunological surveillance in peripheral tissues. Clonal variants use unique T-cell receptors (TCRs) to recognize intracellular pathogens or malignantly transformed cells through cognate interactions with disease-specific peptides presented in class I major histocompatibility complexes (pMHC) on the surface of potential targets. The repertoire of human CD8$^+$ T cells within an individual is estimated to consist of ~$10^6$–$10^8$ different specificities (1). However, only a fraction of these clonal variants recognize and respond to any particular antigen. For example, in chronic HIV infection, HIV Gag-specific CD8$^+$ T cells comprise 0.2–9% of all circulating CD8$^+$ T cells, but in most instances their abundance is less than 2% (2). Characterizing the breadth of epitopes recognized by antigen-specific CD8$^+$ T cells, even ones that represent subdominant populations, is important for understanding immune-mediated control of intracellular infections and for designing and evaluating clinical interventions such as vaccines.

Determining both the breadth of the antigen-specific T-cell response (the range of unique epitopes targeted) and the nature of their functional responses (cytokine secretion, ability to inhibit viral replication, and other functions) is a challenging task. In some cases, the diversity of T-cell epitopes is small: For example, T-cell responses to melanoma usually are well defined (e.g., HLA*A02-restricted MART-1) (3). However, variations in genotypes among the population broaden the immunodominant epitopes induced by most natural infections or by vaccines. The breadth of the CD8$^+$ T-cell response routinely is determined by ELISpot, using first pools of peptides and then individual peptides to confirm specificities (4). Such analysis requires substantial numbers of cells (~$10^6$–$10^7$) and typically measures only a single functional response (secretion of IFN-γ). Significantly, cells identified in these assays cannot be retrieved, and secondary procedures are needed to establish clonal lines with which other biologically relevant functions, such as the ability to inhibit viral replication, can be determined.

The isolation of antigen-specific CD8$^+$ T cells now is commonly performed ex vivo by flow-cytometric sorting using fluorescently labeled recombinant multimers of HLA–peptide complexes to label cells of interest (5). This process minimally requires determining the haplotype of HLAs for a subject. Additionally, the dominant epitopes usually are verified by ELISpot to focus the subsequent analysis with multimeric reagents, which are expensive to produce recombinantly (~$1,000 or more for each one) and have limited varieties of HLA types/epitopes available. Exchanging peptides in the pMHC complexes and using combinatorial sets of labels have improved the scalability and sensitivity of this approach to characterize defined subsets of rare antigen-specific T cells (6, 7), although serial screens for each epitope of interest often are necessary and therefore increase the number of cells required. In aggregate, the total process has a remarkably poor yield (~10–100 unique clones from $10^6$–$10^7$ cells per patient), is labor intensive, and is expensive.

Many clinical studies would benefit from alternative strategies for T-cell cloning that are sample efficient. Quantities of blood from infant and pediatric subjects often are limited, restricting detailed analyses of repertoires. Tissue biopsies also typically yield less than $10^6$ cells, with certain samples, such as cytobrushes or cerebrospinal fluids, containing only ~$10^4$–$10^5$ cells (8, 9). Microscale assays that use microtiter plates or spotted arrays of proteins/peptides have provided alternative means to enumerate antigen-specific T cells from limited numbers of cells but have not enabled routine cloning of identified cells (10–12). More efficient processes for recovering T cells for additional characterization would improve knowledge about the phenotypic and functional diversity of T-cell responses across anatomical sites and patient populations.

We previously demonstrated that dense, elastomeric arrays of "nanowells," microfabricated wells (~$10^5$ per array) with subnanoliter volumes (125 pL), are useful for generating printed microarrays of cytokines released by polyclonally activated human

Author contributions: N.V., D.S.K., and J.C.L. designed research; N.V., D.S.K., K.M.L., A.O.O., M.N.A., and J.M.R. performed research; N.V., D.S.K., K.M.L., A.O.O., M.N.A., and J.C.L. analyzed data; and N.V., D.S.K., B.D.W., and J.C.L. wrote the paper.

Conflict of interest statement: J.C.L. is a founder, shareholder, and consultant of Enumeral Biomedical.

This article is a PNAS Direct Submission.

[1]Present address: Department of Chemical and Biomolecular Engineering, University of Houston, Houston TX 77004.

[2]N.V. and D.S.K. contributed equally.

[3]To whom correspondence should be addressed. E-mail: clove@mit.edu.

This article contains supporting information online at www.pnas.org/lookup/suppl/doi:10.1073/pnas.1111205109/-/DCSupplemental.

T cells (13). This method—called "microengraving"—is based on intaglio printing: A glass slide is temporarily sealed to the array of nanowells to capture analytes secreted by confined cells in both a multiplexed and quantitative manner. This information can guide the recovery of T cells for clonal expansion (14). We also have shown that these arrays of nanowells can enable the concurrent measurement of both cytokine secretion and cytolytic activity to monitor ex vivo cytotoxic T lymphocytes (CTLs) (15).

Here we describe and validate a bioanalytical process that integrates data from both microengraving and on-chip cytometry to identify and recover antigen-specific $CD8^+$ T cells ex vivo from human subjects on the basis of the cytokines secreted following antigen-dependent activation. We demonstrate that the process enumerates cells activated by antigen akin to conventional methods such as ELISpot and intracellular staining (ICS) and allows the detection of HIV-specific $CD8^+$ T cells across a wide range of epitope specificities using samples of limited size ($\sim 10^4$–$10^5$ cells) from blood or tissue. The identified T cells can be retrieved and expanded in vitro for subsequent mapping of fine specificities and detailed functional characterization. The results indicate that this process is highly efficient, with a 100- to 1,000-fold reduction in cells required ex vivo, and should facilitate detailed clonotypic analyses of $CD8^+$ T cells in many areas of human immunology where the numbers of cells are intrinsically small, including tissue biopsies and pediatric samples.

## Results

**Design of Integrated Single-Cell Analysis to Detect Antigen-Specific $CD8^+$ T-Cells ex Vivo.** To establish an efficient method for combined functional characterization ex vivo (cytokine secretion) and in vitro (epitope mapping and inhibition of viral replication), we designed a bioanalytical process to characterize and retrieve antigen-specific $CD8^+$ T cells that also minimizes the total number of cells interrogated. The approach uses an array of nanowells to isolate mononuclear cells after incubation with overlapping pools of peptides (OLPs) or whole antigen (Fig. 1*A*). The array containing cells then is used for multiplexed microengraving to identify antigen-dependent activation of $CD8^+$ T cells. Because analysis by microengraving maintains cell viability, the array of cells can be imaged to enumerate viable $CD8^+$ T cells, and antigen-specific $CD8^+$ T cells can be retrieved by micromanipulation.

**Validation of Process for Enumerating T Cells Activated ex Vivo.** We first tested the ability of our integrated process to determine multifunctional profiles for $CD8^+$ T cells activated ex vivo in a polyclonal manner. Previously frozen peripheral blood mononuclear cells (PBMCs) were thawed and then stimulated for 5 h with *Staphylococcal* enterotoxin B (SEB), a superantigen that stimulates T cells in a Vβ-specific manner. Using unsorted PBMCs minimizes manipulations and allows T cells to average over heterogeneities among antigen-presenting cells (APCs). It also obviates the need for haplotyping a priori to determine suitable HLA-matched APCs. An aliquot of ~200,000 cells in 300 μL then was transferred to the array of nanowells and allowed to settle via gravity for 10 min. The array of cells was rinsed with serum-free medium, placed in contact with a glass slide coated with capture antibodies specific for cytokines commonly associated with $CD8^+$ cytotoxic T-cell responses (TNF, IFN-γ and IL-2), and incubated for 2 h at 37 °C. After incubation, the glass slide was separated from the array of nanowells, washed, and stained with fluorescent antibodies to detect captured cytokines. The cells then were labeled in situ with a viability dye (Calcein AM) and with a fluorescently labeled antibody against CD8. Wells containing single live $CD8^+$ cells were identified by imaging cytometry (Fig. S1) and were matched to the data from those wells corresponding to the cytokines captured by microengraving (Fig. 1*B*). Each experiment/array therefore generated a composite dataset that typically comprised phenotypic profiles for 10,000–30,000 individual live $CD8^+$ cells within a mixed population of mononuclear cells.

We next evaluated our process with clinical samples from subjects chronically infected with HIV-1. There is substantial

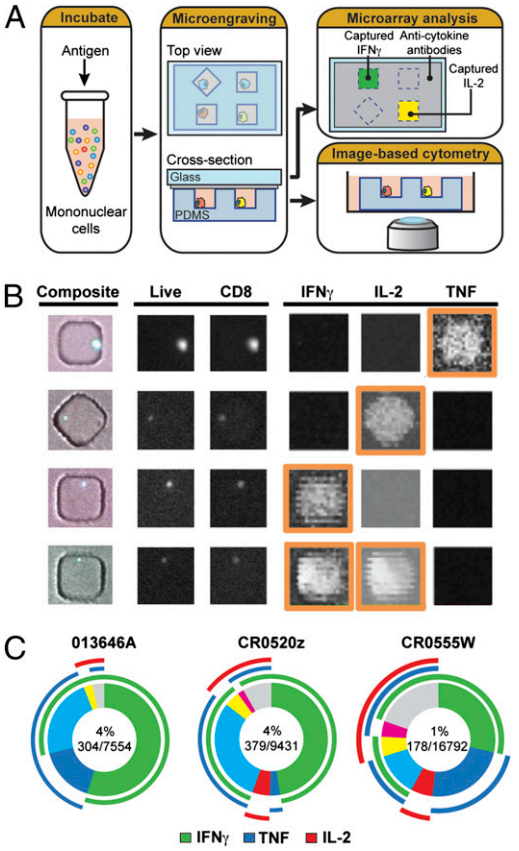


**Fig. 1.** Characterization of multifunctional analysis of $CD8^+$ T cells by microengraving. (*A*) Schematic illustration of approach to measure antigen-specific responses by T cells using a combination of microengraving and imaging cytometry to capture secreted cytokines and enumerate $CD8^+$ T cells. (*B*) Representative composite profiles of individual activated $CD8^+$ T cells. (*C*) Pie charts indicating the relative percentages of T cells secreting one or more cytokines (IFN-γ, green; TNF, blue; IL-2, red) following stimulation with SEB. Cells are from three different $HIV^+$ subjects. Percentages represent the fraction of cells secreting cytokine within the population of single T cells examined.

evidence that HIV-specific $CD8^+$ T-cell responses are essential to the containment of infection in vivo (16). The induction of HIV-specific CTLs is temporally associated with a decline in plasma viremia following acute infection (17, 18), and there are strong correlations between protection from progressive HIV infection and certain HLA class I alleles such as HLA B57, B51, and B27 (19, 20). ELISpot, ICS, and bulk cytolytic assays have shown that HIV-specific $CD8^+$ T cells can produce Tc1-associated cytokines such as IFN-γ, TNF, and IL-2 and eliminate target cells by direct cytolysis upon TCR-mediated recognition of their cognate antigen (21, 22).

We selected a group of $HIV^+$ subjects with varying viral loads (<50–106,000 RNA copies/mL) (Table S1). These subjects included individuals with spontaneously controlled HIV infection in the absence of antiretroviral therapy ("HIV controllers"), those with progressive infection who were not receiving antiretroviral therapy ("chronic progressors"), and individuals receiving anti-HIV drug therapy ("chronic treated"). We first confirmed that these individuals exhibited a range of frequencies of IFN-γ–producing $CD8^+$ T cells specific for the viral protein Gag by ELISpot assays performed against HLA-matched optimal epitopes. The protein Gag was chosen specifically because the breadth, magnitude, and functional capacity of $CD8^+$ T-cell responses toward Gag have been demonstrated to be a reasonable predictor of effective anti-HIV immunity (23, 24).

For three of these subjects, we stimulated PBMCs with SEB for 5 h and profiled the breadth of cytokines secreted by microengraving. A subset of individual $CD8^+$ T cells from all three subjects (1–4%) showed a range of responses, including $CD8^+$ T cells secreting multiple cytokines simultaneously (Fig. 1*C*). The relative distribution of functional responses measured was similar to those determined by ICS, with the most dominant populations producing IFN-γ alone, in combination with either TNF or IL-2 or in combination with IL-2 and TNF together (Fig. S2). Unlike IFN-γ or IL-2, TNF is synthesized initially as a membrane-bound protein that subsequently is cleaved into a soluble form (25). Therefore the higher frequency of cells producing TNF identified by ICS relative to microengraving [regardless of other cytokines those cells may express concurrently, (e.g., more IFN-$\gamma^+$TNF$^+$ production by ICS vs. microengraving)], likely results from the simultaneous detection of both membrane-bound and secreted forms (26). Overall, these results indicate that our process using microengraving to evaluate multifunctional cytokine responses by activated $CD8^+$ T cells is similar to ICS.

**Comparison of Methods for Enumerating Antigen-Dependent $CD8^+$ T Cells ex Vivo.** We next confirmed that our method could detect the activation of $CD8^+$ T cells in an antigen-dependent manner. PBMCs from three HIV-positive individuals were thawed and rested overnight, and their responses were tested against a pool of 66 OLPs (8–10 amino acids each) encompassing the entire Gag protein, an irrelevant melanoma-derived peptide (ELAGIGILTV, EV9) as a negative control, or SEB as a positive control. After incubation with either peptide or SEB for 5 h, the cells were distributed onto an array of nanowells that then was used for microengraving to detect secreted IFN-γ from single, viable $CD8^+$ cells. The data confirmed the ability of our approach to detect antigen-dependent responses consistently for both technical and biological replicates (Fig. 2 *A* and *B*); the frequency of antigen-specific responses ranged from 0.06–0.3%. Using the frequencies of IFN-γ responses measured with the irrelevant peptide, we estimate that the lowest limit of detection possible for the assay is 0.004%, or 1 in 25,000 wells, roughly the same order of magnitude as the number of wells scored. This projected theoretical limit is consistent with a previous estimate we determined for single peptides and antigen-specific activation of CD4 T-cell clones (27) and with that reported for another cell-based microarray for enumerating T cells (12).

We next quantitatively determined the relationships between our microengraving-based process and the two most common techniques used to assess the magnitude of HIV-specific $CD8^+$ T-cell responses—ELISpot and ICS/flow cytometry. Because cells producing IFN-γ were the most abundant population in our polyclonal comparison with ICS, and ELISpot has been well qualified for IFN-γ, we measured the antigen-induced production of IFN-γ from PBMCs isolated from 14 $HIV^+$ individuals. We initially characterized the frequencies of CD4 vs. CD8 T cells in the PBMCs of these patients using flow cytometry (Fig. S3 and Table S1). The frequency of IFN-γ–secreting cells identified by microengraving ranged from 0.04–0.26% when scoring single $CD8^+$ T cells stimulated with a pool of Gag OLPs for 5 h. These results showed a significant correlation with comparable measures obtained by ICS ($P \leq 0.0001$, $r = 0.87$) (Fig. 2*C*) and ELISpot ($P = 0.01$, $r = 0.69$) (Fig. S4). Results obtained by ICS and ELISpot also correlated with each other ($P = 0.01$, $r = 0.90$).

Because the microengraving process can accommodate $10^5$ or fewer cells, we then verified that our method could quantify the frequency of HIV Gag-specific $CD8^+$ T-cell responses from both the peripheral blood and intestinal mucosal compartments of two chronically infected subjects (Fig. 2*D*). These data showed distinct frequencies of HIV-specific responses in each region. Together, these data demonstrate that our microengraving-based process allows the direct ex vivo enumeration of antigen-specific $CD8^+$ T cells from both peripheral and mucosal compartments.

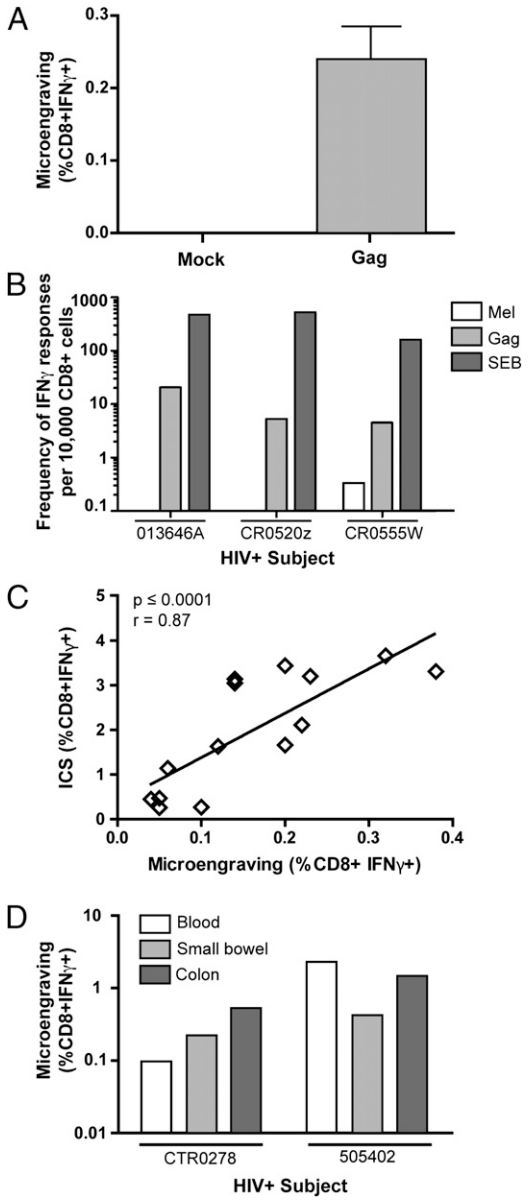


**Fig. 2.** Validation of microengraving for identifying HIV-specific responses. (*A*) Bar graph of the frequencies of IFN-$\gamma^+$ responses scored for $CD8^+$ cells isolated from three different aliquots of PBMCs from the same $HIV^+$ patient stimulated with either a pool of peptides (Gag) or with control medium (Mock). An average of ~6,000 live $CD8^+$ cells were profiled in replicates of each assay. (*B*) Bar graph of the frequencies of IFN-$\gamma^+$ responses scored for $CD8^+$ cells isolated from three different $HIV^+$ subjects. The measurements included stimulation with an irrelevant peptide (melanoma ELAGIGILTV, Mel), a pool of 66 OLPs from Gag, and SEB. An average of ~16,000 live $CD8^+$ cells were profiled in each assay. (*C*) Scatterplots of responses measured from $HIV^+$ subjects by ICS and microengraving. Each diamond indicates one subject. The correlations were assessed by Spearman's rank correlation. (*D*) Assessment of frequencies of HIV Gag-specific $CD8^+$ T-cell responses in blood and mucosal compartments from two chronically infected subjects (CTR0278 and 505402) as assessed by microengraving.

**Rapid and Efficient Cloning of HIV-Specific $CD8^+$ T Cells.** Labeling antigen-specific T cells with recombinant peptide–MHC complexes is useful for recovering T cells with known specificities and relatively high avidities, but it requires a priori knowledge about the haplotype and frequencies of responses of the individual. Antigenic stimulation of cells and analysis by ICS allows the identification of antigen-specific $CD8^+$ T cells ex vivo, but the method renders the cells nonviable. This outcome precludes

further analysis of cells of interest to assess their ability to proliferate in vitro, their ability to inhibit viral replication, or their functional ability to lyse infected cells. Because microengraving is a nondestructive process, and cells have known spatial addresses within the array of wells used, we expected that microengraving would allow the efficient recovery of activated antigen-specific cells by micromanipulation for clonal expansion (Fig. S5) (14, 28).

We identified an HIV controller, CTR0278, who had a detectable Gag-specific IFN-γ response in the peripheral blood but whose $CD8^+$ T cells isolated ex vivo, interestingly, failed to reduce viral replication of an HIV laboratory strain (JRCSF) in vitro. To enable a comparison of the breadth and specificity of Gag-specific cells recovered using our microengraving-based method, we first determined the relative breadth of the HIV-specific $CD8^+$ T cells by ELISpot (Fig. 3*A*). The most abundant Gag-specific responses were directed toward epitopes contained within p17 and p24. We then used microengraving to identify and recover $CD8^+$ T cells secreting IFN-γ from this subject. PBMCs were incubated with pooled OLPs from Gag for 5 h, and the profiles for cytokine secretion were measured using microengraving. In one representative experiment, cells that secreted IFN-γ were enumerated (33 positive events out of 9,925 live $CD8^+$ T cells, 0.33%), and their addresses were determined for subsequent recovery by automated micromanipulation. Experiments with other donors yielded similar numbers of events.

From three independent experiments, we retrieved IFN-$\gamma^+$/$CD8^+$ T cells from 108 wells and then cultivated those single cells in RPMI with irradiated feeder cells, IL-2, and an anti-CD3 antibody to allow efficient clonal expansion. Of these single cells, 93% (100/108) successfully expanded to generate cell lines comprising at least $10^6$ cells, sufficient numbers to run in vitro assays. We then mapped the HIV epitope specificities for 12 of these clonal cell lines by ELISpot. Each of these clones elicited a response to a single Gag OLP or to two adjacent ones contained within the original pool and subsequently also responded to an HLA-matched optimal peptide contained within the mapped OLP(s) (Table S2). Although the small number of characterized clonal cell lines precludes quantitative comparisons between frequencies of responses in PBMCs and the clonal lines established, the clones covered all five optimal responses identified by ELISpot from PBMCs including one (Cw8-RV9) that was near the lower limit of detection for those assays (~60 spot-forming units per $10^6$ cells) (Fig. 3*B*). This result confirms that the microengraving-based method enumerates a broad range of responses and suggests that extended depth of analysis or expanded recovery may identify other clonotypic variants below the limit of detection of ELISpot.

The clonal lines also were tested to determine their capacity to inhibit viral replication in vitro (Fig. 4). Although the complete pool of $CD8^+$ T cells isolated ex vivo failed to inhibit viral replication, individual isolated clonal lines showed varying degrees of viral inhibition. A clone specific for HLA-A2-FK10 was unable to inhibit viral replication, despite induction of IFN-γ by the cognate peptide in ELISpot assays, whereas a clone specific for HLA-A2-SL9 exhibited a 3-log reduction in a p24 ELISA-based viral-inhibition assay. Clones with specificities against HLA-B14-DA9 and against HLA-Cw8-RV9 showed intermediate levels of inhibition. Thus, although bulk $CD8^+$ T cells failed to inhibit viral replication significantly, lines with single epitope specificities derived from the bulk population showed significant antiviral activity, further underscoring the importance of broadly profiling the diversity of T-cell responses from patients.

## Discussion

We have demonstrated a rapid, inexpensive, and efficient process for combining ex vivo and in vitro functional characterization of HIV-specific $CD8^+$ T cells. The time required for executing the process and isolating cells on the basis of phenotype is less than 24 h. The cost per assay is comparable to that for performing a single 96-well plate ELISpot, and the assay can accommodate small samples (10,000–100,000 cells or fewer) easily. The microengraving-based method used has a sensitivity and specificity similar to ELISpot for evaluating antigen-specific responsiveness but also measures multifunctional responses without rendering cells nonviable.

The enumeration of IFN-$\gamma^+$ CD8 T cells following antigenic stimulation as determined by microengraving correlated well with responses determined by both ICS and ELISpot. The magnitude of the responses, however, was more similar to that measured by ELISpot; ICS estimated approximately 10-fold more events. Both ELISpot and microengraving measure proteins secreted in a paracrine manner by viable cells, whereas ICS measures total protein synthesized by rendering cells nonviable. Indeed, previous reports comparing the magnitude of virus-specific responses (to HIV/cytomegalovirus/simian immunodeficiency virus) measured

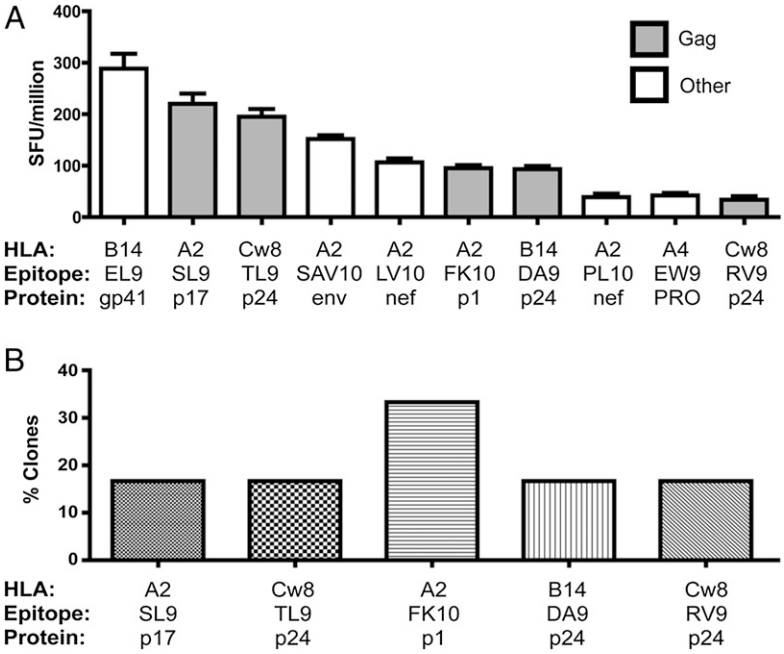


**Fig. 3.** Dominant epitopes recognized by $CD8^+$ T cells from an elite controller. (*A*) Rank-ordered bar graph of the most frequent responses measured by ELISpot, and organized by epitope, among $CD8^+$ T cells from elite controller CTR0278 run in triplicate. Filled bars indicate Gag-specific responses. (*B*) Bar graph of the frequencies of T-cell clones recognizing specific epitopes in gag identified by microengraving and recovered by micromanipulation. SFU, spot-forming units.

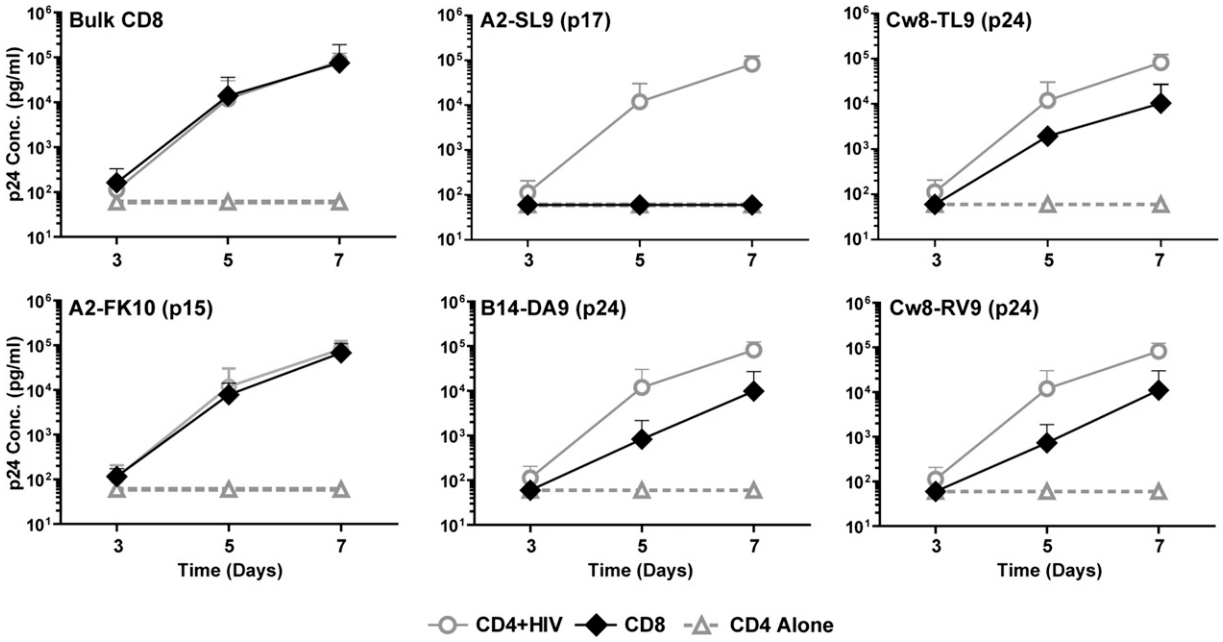


**Fig. 4.** In vitro viral-inhibition assays. Representative results from each of the five different epitopes identified via microengraving and the bulk CD8$^+$ T cells from sample CTR0278, showing inhibition of viral replication over 7 d of culture. Open circles represent autologous activated CD4$^+$ T cells infected with HIV-1 strain JRCSF; closed diamonds represent CD4/CD8 cocultures; open triangles represent CD4$^+$ T cells without superinfection with HIV-1 strain JRCSF. Each experiment was run in triplicate. Error bars represent SD.

by ELISpot and ICS in both humans and macaques have demonstrated that the magnitude of responses determined via ELISpot is consistently lower than that of responses determined via ICS—findings that agree with those observed here for both ELISpot and microengraving (29–31). The limited window of measurement afforded in microengraving relative to integrated ICS also may affect the lower number of events enumerated (32).

The ability to recover and expand by microengraving individual identified HIV-specific cells that may have functional significance in vivo despite poor detection in bulk assays should help refine our understanding of effective T-cell–mediated immune responses in one or more anatomical compartments (33). HIV-specific CD8$^+$ T cells are important for the control of viremia, but the critical functions performed by these cells that contribute to control remain unknown (34, 35). More complex functions, such as proliferation or simultaneous expression of multiple cytokines, may better identify effective CD8$^+$ cytotoxic T lymphocytes (36, 37). The ability of CTLs to recognize and kill virus-infected cells may be critical for mediating control in vivo, and it may be crucial to evaluate these functions comprehensively in vitro (38). We show that functional characterization of individual clones by in vitro viral-inhibition assays can identify functionality linked to single epitopes not detected by similar bulk assays. It also should allow a straightforward approach to investigate the role of TCR use in functional CTL activity based on the TCR sequences of identified clones.

One significant advantage afforded by the enhanced efficiency of the microengraving-based approach for recovering antigen-specific T cells should be its application in monitoring responses when clinical samples simply have sparse numbers of cells, such as mucosal tissues, pediatric blood samples, or genital secretions. The microengraving-based approach also allows a less biased assessment of immune targeting than other currently available approaches. It does not require a priori knowledge of haplotypes and accommodates diverse sources of antigen, including whole proteins or even pathogens. In this way, broad coverage of the T-cell response can be assessed in an initial screen. The method shifts the burden of establishing epitope specificity to the expanded clones, but for small samples, detailed analysis to determine specificity may be determined more effectively when more cells are available after expansion. In our screen of the T-cell response from an HIV controller, we recovered representative clones for each of the most abundant specificities determined by ELISpot from only a small pool of those generated. Increasing the number of clones sampled and subsequent analyses of those clones should enable broad coverage of the T-cell response. The ability to establish clonal lines also should allow additional characterization, such as the determination of clonotypes and proliferative capacity (39).

In conclusion, this bioanalytical process establishes a rapid and efficient approach for cloning primary antigen-specific T cells and will provide opportunities to characterize HIV-specific responses, among others. In particular, we expect that it will be useful when the number of cells available is insufficient for extensive analysis by standard techniques or when it is critical to assess antigenic coverage broadly with minimal bias. The application of this technique should inform studies of HIV pathogenesis as well as aid the assessment of potential HIV vaccine candidates and has broad relevance to other areas of immunology.

## Materials and Methods

**Patient Samples.** HIV-infected individuals were enrolled at Massachusetts General Hospital in accordance with institutional review board-approved protocols. PBMCs were isolated from blood by Ficoll (Sigma) density purification in accordance with the manufacturer's instructions. Fresh or frozen PBMCs were used subsequently for the described experiments. Mucosal biopsies from the small bowel and colon were obtained by endoscopy, and a matching blood sample was obtained the same day. Biopsy samples were disaggregated with collagenase, as described previously (40).

**Fabrication of Nanowell Arrays.** Arrays of 1-mm-thick polydimethylsiloxane nanowells (50 μm) were manufactured by replica molding using a custom-built mold, adhered directly to a 3 in ×1 in glass slide, and sterilized in an oxygen plasma before use (41).

**Activation and Deposition of Cells.** Experiments were performed with frozen PBMCs that were thawed and rested overnight (12–16 h) or with fresh mononuclear cells from blood and intestinal biopsies. An aliquot of $1 \times 10^6$ cells in 500 μL of R10 (RPMI + 10% FBS) was stimulated with SEB or with a pool of 66 OLPs (8–10 amino acids each; 2 μg/mL) encompassing the entire Gag protein (or ELAGIGILTV as a control) along with the costimulatory antibodies

anti-CD28 and anti-CD49d for 5 h. Stimulated cells were counted and adjusted to a density of $1 \times 10^6$ cells/mL A 300-μL aliquot of the cells was deposited onto a sterilized array of nanowells. The cells settled via sedimentation for 10 min and were then examined by microscopy to estimate the frequency of loading (approximately one cell per well). Excess cells were removed by rinsing the array gently with medium and subsequent aspiration.

**Microengraving and On-Chip Cytometry.** The cell-loaded array was washed with serum-free medium containing 5 ng/mL of IgG (to facilitate registration of the nanowell array to the printed microarray). A polylysine-functionalized glass was preincubated for 1 h with capture antibodies against IFN-γ, TNF-α, IL-2, and Ig (25 μg/mL each). The slide was blocked with 3% milk/PBS-Tween (0.05%, PBST), washed twice with PBST, and dried. The nanowell array was held in contact with the glass slide under compression in a hybridization chamber (Agilent) and incubated (37 °C, 5% $CO_2$) for 2 h. After incubation, the glass slide was separated from the nanowell array, washed, and labeled with the appropriate fluorescent antibodies, as described previously (41). The printed microarrays were imaged using a Genepix 4200AL (MDS Corp.). The array of cells subsequently was labeled in situ with Calcein violet live cell marker (1 μM; Invitrogen) and a fluorescent antibody against CD8 (5μg/mL each) and then was incubated in the dark for 30 min. The array was imaged by epifluorescence on an automated microscope (Zeiss). The data from microengraving and the on-chip cytometry were matched on a per-well basis for individual viable CD8 cells.

**Retrieval and Expansion of T Cells.** $CD8^+IFN\text{-}\gamma^+$ T cells were retrieved using an automated micromanipulator (CellCelector; AVISO GmbH) (28). Retrieved cells were incubated in a well of a 96-well plate with 200 μL of R10 supplemented with 100 U/mL of IL-2 (R10/100) containing irradiated (2,500 cGy) HLA-mismatched PBMCs ($10^6$/mL) from an $HIV^-$ donor (42). Cells were stimulated with anti-CD3 antibody (clone 12F6), and irradiated feeder cells were added every 2 wk over the course of approximately 2 mo. During this time, cells were expanded to larger volumes until there were sufficient cells available for functional assays (at least $10^6$ cells).

**Additional Methods.** Additional descriptions of methods, including fabrication of nanowells, functionalization of glass, intracellular staining, ELISpot, and viral-inhibition assays, are available in *SI Materials and Methods*.

**ACKNOWLEDGMENTS.** This research was supported by the Charles A. Dana Foundation, the W. M. Keck Foundation, and the Ragon Institute of Massachusetts General Hospital, Massachusetts Institute of Technology, and Harvard University. N.V. received support from National Institute of Allergy and Infectious Diseases/National Institutes of Health GrantU54-AI057156. D.S.K. is supported by a National Institutes of Health Mentored Clinical Scientist Development Award (K08) and the Burroughs Wellcome Fund. A.O.O. was supported in part by National Institutes of Health Biotechnology Training Fellowship NIGMS 5T32GM008334 and by a United Negro College Fund–Merck Graduate Science Research Dissertation Fellowship. J.C.L. is a Latham Family Career Development Professor.

1. Robins HS, et al. (2010) Overlap and effective size of the human CD8+ T cell receptor repertoire. *Sci Transl Med* 2(47):47–64.
2. Betts MR, et al. (2001) Analysis of total human immunodeficiency virus (HIV)-specific CD4(+) and CD8(+) T-cell responses: Relationship to viral load in untreated HIV infection. *J Virol* 75:11983–11991.
3. Ellis JM, et al. (2000) Frequencies of HLA-A2 alleles in five U.S. population groups. Predominance Of A*02011 and identification of HLA-A*0231. *Hum Immunol* 61: 334–340.
4. Streeck H, Frahm N, Walker BD (2009) The role of IFN-gamma Elispot assay in HIV vaccine research. *Nat Protoc* 4:461–469.
5. Altman JD, Davis MM (2003) MHC-peptide tetramers to visualize antigen-specific T cells. *Curr Protoc Immunol* 53:17.3.1–17.3.33.
6. Toebes M, Rodenko B, Ovaa H, Schumacher TN (2009) Generation of peptide MHC class I monomers and multimers through ligand exchange. *Curr Protoc Immunol* 87: 18.16.1–18.16.20.
7. Rodenko B, et al. (2006) Generation of peptide-MHC class I complexes through UV-mediated ligand exchange. *Nat Protoc* 1:1120–1132.
8. Subirá D, et al. (2002) Flow cytometric analysis of cerebrospinal fluid samples and its usefulness in routine clinical practice. *Am J Clin Pathol* 117:952–958.
9. Martin-Hirsch P, Jarvis G, Kitchener H, Lilford R (2000) Collection devices for obtaining cervical cytology samples. *Cochrane Database Syst Rev* (3):CD001036.
10. Li Pira G, Ivaldi F, Bottone L, Manca F (2007) High throughput functional microdissection of pathogen-specific T-cell immunity using antigen and lymphocyte arrays. *J Immunol Methods* 326:22–32.
11. Hoff A, et al. (2010) Peptide microarrays for the profiling of cytotoxic T-lymphocyte activity using minimum numbers of cells. *Cancer Immunol Immunother* 59:1379–1387.
12. Yue C, Oelke M, Paulaitis ME, Schneck JP (2010) Novel cellular microarray assay for profiling T-cell peptide antigen specificities. *J Proteome Res* 9:5629–5637.
13. Bradshaw EM, et al. (2008) Concurrent detection of secreted products from human lymphocytes by microengraving: Cytokines and antigen-reactive antibodies. *Clin Immunol* 129:10–18.
14. Han Q, Bradshaw EM, Nilsson B, Hafler DA, Love JC (2010) Multidimensional analysis of the frequencies and rates of cytokine secretion from single cells by quantitative microengraving. *Lab Chip* 10:1391–1400.
15. Varadarajan N, et al. (2011) A high-throughput single-cell analysis of human $CD8^+$ T cell functions reveals discordance for cytokine secretion and cytolysis. *J Clin Invest* 121:4322–4331.
16. Deeks SG, Walker BD (2007) Human immunodeficiency virus controllers: Mechanisms of durable virus control in the absence of antiretroviral therapy. *Immunity* 27: 406–416.
17. Koup RA, et al. (1994) Temporal association of cellular immune responses with the initial control of viremia in primary human immunodeficiency virus type 1 syndrome. *J Virol* 68:4650–4655.
18. Borrow P, Lewicki H, Hahn BH, Shaw GM, Oldstone MB (1994) Virus-specific CD8+ cytotoxic T-lymphocyte activity associated with control of viremia in primary human immunodeficiency virus type 1 infection. *J Virol* 68:6103–6110.
19. Dyer WB, et al. (2008) Mechanisms of HIV non-progression; robust and sustained CD4+ T-cell proliferative responses to p24 antigen correlate with control of viraemia and lack of disease progression after long-term transfusion-acquired HIV-1 infection. *Retrovirology* 5:112.
20. Pereyra F, et al.; International HIV Controllers Study (2010) The major genetic determinants of HIV-1 control affect HLA class I peptide presentation. *Science* 330: 1551–1557.
21. Chen H, et al. (2009) Differential neutralization of human immunodeficiency virus (HIV) replication in autologous CD4 T cells by HIV-specific cytotoxic T lymphocytes. *J Virol* 83:3138–3149.
22. Sun Y, et al. (2003) A systematic comparison of methods to measure HIV-1 specific CD8 T cells. *J Immunol Methods* 272:23–34.
23. Zuñiga R, et al. (2006) Relative dominance of Gag p24-specific cytotoxic T lymphocytes is associated with human immunodeficiency virus control. *J Virol* 80:3122–3125.
24. Kiepiela P, et al. (2007) CD8+ T-cell responses to different HIV proteins have discordant associations with viral load. *Nat Med* 13:46–53.
25. Moss ML, et al. (1997) Cloning of a disintegrin metalloproteinase that processes precursor tumour-necrosis factor-alpha. *Nature* 385:733–736.
26. Haney D, et al. (2011) Isolation of viable antigen-specific CD8+ T cells based on membrane-bound tumor necrosis factor (TNF)-α expression. *J Immunol Methods* 369: 33–41.
27. Song Q, et al. (2010) On-chip activation and subsequent detection of individual antigen-specific T cells. *Anal Chem* 82:473–477.
28. Choi JH, et al. (2010) Development and optimization of a process for automated recovery of single cells identified by microengraving. *Biotechnol Prog* 26:888–895.
29. Karlsson AC, et al. (2003) Comparison of the ELISPOT and cytokine flow cytometry assays for the enumeration of antigen-specific T cells. *J Immunol Methods* 283: 141–153.
30. Pahar B, Li J, Rourke T, Miller CJ, McChesney MB (2003) Detection of antigen-specific T cell interferon gamma expression by ELISPOT and cytokine flow cytometry assays in rhesus macaques. *J Immunol Methods* 282:103–115.
31. Maecker HT, et al. (2005) Impact of cryopreservation on tetramer, cytokine flow cytometry, and ELISPOT. *BMC Immunol* 6:17.
32. Han Q, et al. (2012) Polyfunctional responses by human T cells result from sequential release of cytokines. *Proc Natl Acad Sci USA* 109:1605–1612.
33. Schaubert KL, et al. (2010) Generation of robust CD8+ T-cell responses against subdominant epitopes in conserved regions of HIV-1 by repertoire mining with mimotopes. *Eur J Immunol* 40:1950–1962.
34. Addo MM, et al. (2003) Comprehensive epitope analysis of human immunodeficiency virus type 1 (HIV-1)-specific T-cell responses directed against the entire expressed HIV-1 genome demonstrate broadly directed responses, but no correlation to viral load. *J Virol* 77:2081–2092.
35. Dalod M, et al. (1999) Broad, intense anti-human immunodeficiency virus (HIV) ex vivo CD8(+) responses in HIV type 1-infected patients: Comparison with anti-Epstein-Barr virus responses and changes during antiretroviral therapy. *J Virol* 73:7108–7116.
36. Betts MR, et al. (2006) HIV nonprogressors preferentially maintain highly functional HIV-specific CD8+ T cells. *Blood* 107:4781–4789.
37. Migueles SA, et al. (2002) HIV-specific CD8+ T cell proliferation is coupled to perforin expression and is maintained in nonprogressors. *Nat Immunol* 3:1061–1068.
38. Sáez-Cirión A, et al. (2009) ANRS EP36 HIV Controllers Study Group (2009) Heterogeneity in HIV suppression by CD8 T cells from HIV controllers: Association with Gag-specific CD8 T cell responses. *J Immunol* 182:7828–7837.
39. Billam P, et al. (2011) T Cell receptor clonotype influences epitope hierarchy in the CD8+ T cell response to respiratory syncytial virus infection. *J Biol Chem* 286: 4829–4841.
40. Shacklett BL, et al. (2003) Optimization of methods to assess human mucosal T-cell responses to HIV infection. *J Immunol Methods* 279:17–31.
41. Han C, et al. (2010) Integration of single oocyte trapping, in vitro fertilization and embryo culture in a microwell-structured microfluidic device. *Lab Chip* 10:2848–2854.
42. Yang OO, et al. (1997) Suppression of human immunodeficiency virus type 1 replication by CD8+ cells: Evidence for HLA class I-restricted triggering of cytolytic and noncytolytic mechanisms. *J Virol* 71:3120–3128.

# Supporting Information

## Varadarajan et al. 10.1073/pnas.1111205109

### SI Materials and Methods

**Clinical Groups.** Individuals were grouped according to clinical parameters as follows: HIV controllers [HIV-1 viral load <2,000 RNA copies/mL in the absence of antiretroviral therapy (ART)], chronic untreated (HIV-1 viral load >2,000 RNA copies/mL not receiving ART), and chronic treated (HIV-1 viral load <50 copies/mL receiving ART).

**Fabrication of Nanowell Arrays.** The nanowell arrays were fabricated using a combination of photolithography and replica molding, as described previously (1). Briefly, a silicon wafer supporting a pattern of SU-8 photoresist was prepared by photolithography and used as a template for molding. Nanowell arrays were produced by casting a biocompatible elastomer (polydimethylsiloxane, PDMS; 10:1 base:catalyst; Dow Corning) on this template and curing at 80 °C for 2 h. Each array comprising 72 × 24 blocks of wells was 1 mm thick and adhered directly to a 3 in ×1 in glass slide. In this study, the arrays comprised blocks of 7 × 7 nanowells with dimensions of 50 μm × 50 μm × 50 μm (with a center-to-center distance of 100 μm) for a total of 84,672 wells per array. Before use, the array was sterilized and rendered hydrophilic by treatment with an oxygen plasma (Harrick).

**Preparation of Glass Slides for Microengraving.** Functionalized glass slides were prepared as described (2). Briefly, poly-L-lysine–coated slides were incubated with 10 μg/mL of each capture antibody [IFN-γ (1-D1K; Mabtech), IL-2 (MAB602; R&D), TNF-α (MAb1; Biolegend), and human IgG (81-7100; Invitrogen)] for 1 h at 25 °C and then were stored at 4 °C until use. Borate buffer (pH 9) was used for diluting antibodies (3). Before microengraving, coated slides were blocked with 3% nonfat milk in PBS for 30 min, washed three times with PBS, and spun dry.

**Intracellular Cytokine Staining.** Intracellular staining (ICS) was performed as previously reported (4). Frozen peripheral blood mononuclear cells (PBMCs) were thawed and rested overnight. Then $1 \times 10^6$ cells in 1 mL of fresh R10 were transferred to 5-mL polycarbonate tubes and incubated with costimulatory antibodies (anti-CD28 and anti-CD49d) just before stimulation with the following conditions: no peptide (negative control), Gag overlapping peptides (OLPs) (0.5 μg/mL), and *Staphylococcus* endotoxin B (SEB) (0.25 μg/mL; positive control). After incubation at 37 °C for 1 h, brefeldin A was added at a concentration of 5 μg/mL, and the cells were transferred to an incubator (37 °C/5% $CO_2$) for 14 h. Cells then were washed with PBS, labeled first with viability dye (Invitrogen) for 30 min and stained for 15 min with the following fluorochrome-conjugated antibodies: CD3-APC H7, CD4-PerCP, CD8-APC, and CD14/19-Pacific Blue (BD Biosciences). The cells then were washed and permeabilized and labeled intracellularly with anti–IL-2-FITC, anti–IFN-γ-PE Cy7, and anti–TNF-α-Alexa 700 (BD Biosciences). Cells then were washed again and analyzed on an LSRII flow cytometer (BD Biosciences).

**ELISpot.** Briefly, frozen PBMCs were thawed and rested overnight, and $10^5$ cells in 200 uL of R10 were loaded onto each well of a 96-well plate precoated with anti–human IFN-γ monoclonal antibody (2 μg/mL). Cells then were stimulated with Gag OLPs (14 μg/mL) and incubated overnight. Cells were stimulated separately with phytohemagglutinin (1.25 μg/mL) or no peptide as appropriate positive and negative controls. The plates then were incubated with a biotinylated IFN-γ secondary antibody (30 min) and then with streptavidin-alkaline phosphatase (30 min) and were developed colorimetrically. The frequencies of the responses are reported as the background-corrected spot-forming units per million PBMCs. A response at least two SDs above background was considered a positive response.

ELISpot also was used to map specificities of expanded clonal cells lines. These experiments were carried out as above, except that $5 \times 10^4$ cells were assessed in each well of a 96-well plate. Individual Gag peptides from the OLP pool (66 individual peptides total) or HLA-matched optimal Gag peptides were used to stimulate the lines. Positive responses were determined to be lines that demonstrated >400 spots per well (in all cases too numerous to count).

**Viral-Inhibition Assay.** Assays were performed as previously described (5). Autologous $CD4^+$ T cells were negatively enriched from PBMCs using Dynal magnetic bead separation (Invitrogen; 15 uL per $10^6$ cells) and activated with anti-CD3.8 antibody (0.5 μg/mL) in R10/50 for 3 d. Activated $CD4^+$ T cells were infected with HIV-1 strain JRCSF at a multiplicity of infection of 0.05 for 4 h and were washed with R10. Then $1 \times 10^5$ HIV-exposed cells were plated with bulk CD8 or Gag-specific CD8 clones at a ratio of 1:1 in 200 uL of R10/50. Infected and noninfected CD4 cells were cultured by themselves as positive and negative controls, respectively. HIV replication was assessed by p24 ELISA (Perkin-Elmer) with culture supernatants at day 3, 5, and 7.


1. Ogunniyi AO, Story CM, Papa E, Guillen E, Love JC (2009) Screening individual hybridomas by microengraving to discover monoclonal antibodies. *Nat Protoc* 4:767–782.
2. Han Q, Bradshaw EM, Nilsson B, Hafler DA, Love JC (2010) Multidimensional analysis of the frequencies and rates of cytokine secretion from single cells by quantitative microengraving. *Lab Chip* 10:1391–1400.
3. Ronan JL, Story CM, Papa E, Love JC (2009) Optimization of the surfaces used to capture antibodies from single hybridomas reduces the time required for microengraving. *J Immunol Methods* 340:164–169.
4. Nomura L, Maino VC, Maecker HT (2008) Standardization and optimization of multiparameter intracellular cytokine staining. *Cytometry A* 73:984–991.
5. Yang OO, et al. (1997) Suppression of human immunodeficiency virus type 1 replication by CD8+ cells: Evidence for HLA class I-restricted triggering of cytolytic and noncytolytic mechanisms. *J Virol* 71:3120–3128.

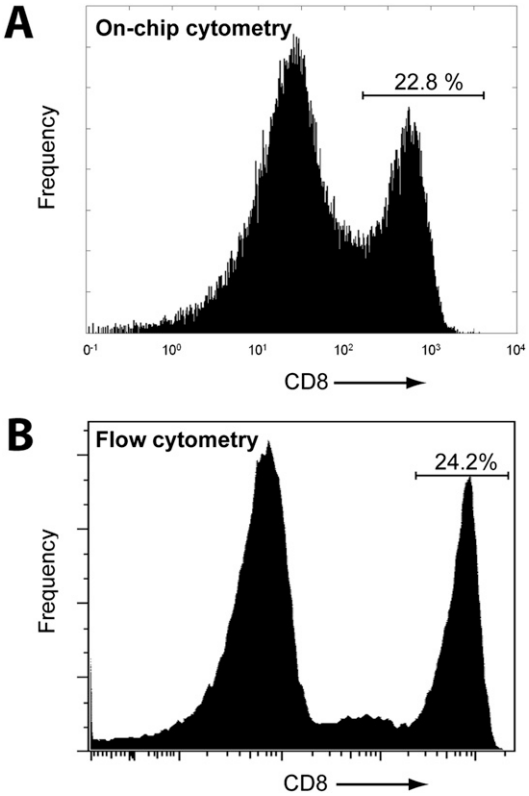


**Fig. S1.** Histograms of the distribution of PBMCs expressing CD8 as determined by on-chip imaging cytometry (*A*) and comparative analysis by flow cytometry (*B*).

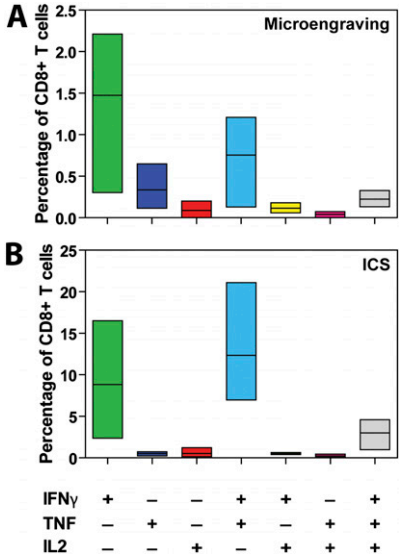


**Fig. S2.** Box plots of the relative distributions of functional responses measured for SEB-activated T cells by microengraving (*A*) and by ICS (*B*) ($n$ = 3).

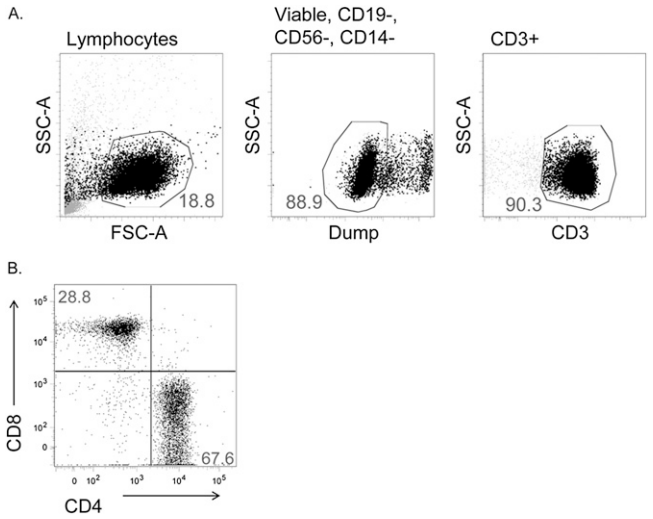


**Fig. S3.** Representative flow cytometry plots of the gating strategy used to identify (*A*) $CD3^+$ cells and (*B*) $CD3^+$ $CD8^+$ and $CD3^+CD4^+$ cells.

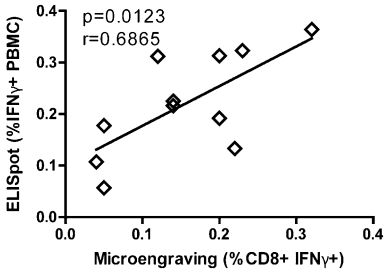


**Fig. S4.** Scatterplots of responses measured from $HIV^+$ subjects by ELISpot and microengraving. Each diamond indicates one subject. Correlations were assessed by Spearman's rank correlation.

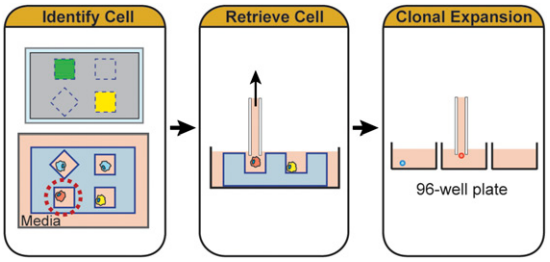


**Fig. S5.** Schematic illustration of the enumeration of IFN-$\gamma^+$ $CD8^+$ cells by microengraving and subsequent retrieval by micromanipulation.

**Table S1. Clinical parameters for HIV$^+$ subjects used for microengraving with CD4$^+$ and CD8$^+$ T-cell percentage as determined by flow cytometry**

| Patient ID | Sex | Age | Race | Classification | Viral load (copies/mL) | CD4$^+$ T-cell count (cells/μL) | CD8% | CD4% |
|---|---|---|---|---|---|---|---|---|
| CR0648z | Male | 41 | White | Treated | <50 | 649 | 58.1 | 36.5 |
| CR0712Y | Male | 40 | White | Treated | <50 | 791 | 47.2 | 40.7 |
| 013113J | Male | 43 | African American | Untreated | 10,6000 | 230 | 68.6 | 22.2 |
| 505402 | Male | 37 | White | Untreated | 39,795 | 807 | 53.2 | 39.8 |
| CR0541v | Male | 31 | African American | Untreated | 4,240 | 320 | 50.1 | 44.9 |
| CR0555w | Female | 34 | White | Untreated | 24,400 | 875 | 53.9 | 40.6 |
| FEN007 | Male | 45 | African American | Untreated | 1,420 | 510 | 45.1 | 51.1 |
| 013646a | Male | 45 | White | Controller | <50 | 871 | 22.0 | 75.3 |
| CR0462R | Male | 26 | White | Controller | <50 | 1290 | 37.3 | 57.0 |
| CR0509m | Male | 45 | African American | Controller | 3,740 | 364 | 50.5 | 36.3 |
| CR0520z | Male | 38 | White | Controller | 929 | 1181 | 32.3 | 61.6 |
| CR0559m | Male | 47 | White | Controller | <50 | 1026 | 40.6 | 55.2 |
| CR0757 | Male | 44 | White | Controller | 10,800 | 1041 | 33.6 | 62.1 |
| CR0772T | Male | 40 | African American | Controller | <50 | 696 | 28.8 | 67.6 |
| CTR0174 | Male | 46 | African American | Controller | 110 | 1024 | 43.0 | 49.5 |
| CTR0278c | Female | 51 | White | Controller | 252 | 271 | 63.8 | 28.3 |
| FW23 | Male | 49 | White | Controller | 1,104 | 829 | 30.2 | 63.3 |

**Table S2. Fine epitope specificities of 12 CD8$^+$ T-cell clones identified from an HIV$^+$ elite controller by microengraving**

| Clone number | Gag OLP | Optimal peptide | HLA allele | Protein |
|---|---|---|---|---|
| CTR0278.1 | 41, 42 | REPWDEWVV | Cw8 | p24 |
| CTR0278.2 | 59 | FLGKIWPSYK | A2 | p15 |
| CTR0278.3 | 59 | FLGKIWPSYK | A2 | p15 |
| CTR0278.4 | 41 | DRFYKTLRA | B14 | p24 |
| CTR0278.5 | 59 | FLGKIWPSYK | A2 | p15 |
| CTR0278.6 | 59 | FLGKIWPSYK | A2 | p15 |
| CTR0278.7 | 11, 12 | SLYNTVATL | A2 | p17 |
| CTR0278.8 | 41 | DRFYKTLRA | B14 | p24 |
| CTR0278.9 | 41, 42 | REPWDEWVV | Cw8 | p24 |
| CTR0278.10 | 11, 12 | SLYNTVATL | A2 | p17 |
| CTR0278.11 | 25 | TPQDLNTML | Cw8 | p24 |
| CTR0278.12 | 25 | TPQDLNTML | Cw8 | p24 |